Optimizing the Repeatability of Choriocapillaris Flow Deficit Measurement From Optical Coherence Tomography Angiography

IKSOO BYON, AHMED ROSHDY ALAGORIE, YONGSOK JI, LI SU, AND SRINIVAS R. SADDA

• PURPOSE: To evaluate the impact of processing technique and slab selection on the repeatability of choriocapillaris (CC) flow deficit (FD) measurements as assessed using optical coherence tomography angiography (OCTA)

• DESIGN: Prospective, cross-sectional study.

• METHODS: Healthy subjects were imaged with 4 consecutive 3 × 3-mm OCTA using a swept-source OCT (PLEX elite 9000; Carl Zeiss Meditec). OCTA images were generated using the Max projection, and three 10-μm-thick slabs starting 11, 21, and 31 μm posterior to the automatically segmented retinal pigment epithelial band. The resultant images were binarized using the Phansalkar method with a 43.94-μm radius and then the CCFD% was computed. The intraclass correlation coefficient (ICC) and coefficient of variation (CV) were computed for the 4 acquisitions to assess the repeatability of the CCFD%. This entire analysis was repeated after separately modulating several parameters: (1) Sum instead of the Max projection, (2) retinal pigment epithelial fit instead of the retinal pigment epithelial band as the offset reference, (3) 14.65 and 87.88 μm radius values instead of 43.94 μm.

• RESULTS: Twenty-four healthy eyes (mean age; 36.4 years) were enrolled. The CCFD% in the 11-21-, 21-31-, and 31-41-μm slabs generated by the Max algorithm and the retinal pigment epithelial band showed high repeatability values (ICCs = 0.963, 0.975, and 911; CVs = 0.05, 0.05, and 0.05, respectively). As most of the cases were confounded with the hypointense region when the 11-21-μm slab was used, however, this slab could not be included in the subsequent analyses. Those values in the 21-31- and 31-41-μm slabs were higher than those of the corresponding slabs by the Sum algorithm (ICC = 0.916 and 0.776; CV = 0.15 and 0.19, respectively) or by the retinal pigment epithelial fit (ICC = 0.907 and 0.802; CV = 0.06 and 0.06, respectively). The Phansalkar radius of 43.94 μm had the highest ICC numerically, but this was not statistically significantly greater than for a radius of 14.65 μm (ICC = 0.960 and 0.911, respectively) or a radius of 87.88 μm (ICC = 0.958 and 0.897, respectively). Regardless of which parameter was modulated, the 21-31-μm slab was the most repeatable.

• CONCLUSIONS: In normal eyes, en face CC OCTA images generated using the Max projection and a 10-μm-thick slab offset of 21 μm below the instrument-generated retinal pigment epithelial band yielded the most repeatable CCFD%. These findings have implications for the design of standardized processing algorithms for quantitative CC assessment. (Am J Ophthalmol 2020;219:21–32. © 2020 Elsevier Inc. All rights reserved.)

OPTICAL COHERENCE TOMOGRAPHY ANGIOGraphy (OCTA) is a noninvasive imaging technology that allows visualization of the retinal and inner choroidal microcirculation. The availability of commercial swept-source (SS) OCT devices with a longer-wavelength light source (1060 nm) and higher scan speed (100-200K A-scans per second) has further enhanced the imaging capability of OCTA, in particular allowing better penetration of signal below the retinal pigment epithelium, which may be problematic in the setting of pathology with spectral-domain OCT or with conventional dye-based angiography.[1,2] A significant advantage of OCTA over dye-based angiography is that its high axial resolution allows the 3-dimensional organization of the retinal circulation and choriocapillaris (CC) to be resolved.[3,4] In addition, the high contrast of OCTA lends itself to quantification using simple binarization techniques in which pixels of an image are divided into pixels with flow or without flow. This allows a variety of parameters such as vessel density, vessel diameter index, and flow deficit (FD) to be computed.[5–9]

The CC is the capillary circulation of the choroid and is located below the retinal pigment epithelium and Bruch membrane. The CC is a thin, dense, compact vascular

Accepted for publication May 18, 2020.

From the Doheny Image Reading Center, Doheny Eye Institute (I.B., A.R.A., Y.J., L.S., S.R.S.), Los Angeles, California, USA; Department of Ophthalmology, David Geffen School of Medicine at UCLA (I.B., A.R.A., Y.J., L.S., S.R.S.), Los Angeles, California, USA; Department of Ophthalmology, Biomedical Research Institute, Pusan National University Hospital, Pusan National University School of Medicine (I.B.), Busan, South Korea; Department of Ophthalmology, Faculty of Medicine, Tanta University (A.R.A.), Tanta, Egypt; Department of Ophthalmology, Chonnam National University Medical School and Hospital (Y.J.), Gwangju, South Korea; and Department of Ophthalmology, Shanghai General Hospital (Shanghai First People's Hospital), Shanghai Jiao Tong University School of Medicine (L.S.), Shanghai, China.

Inquiries to Srinivas R. Sadda, 1355 San Pablo Street, Suite 211, Los Angeles, CA 90033, USA; e-mail: ssadda@doheny.org

0002-9394/$36.00
https://doi.org/10.1016/j.ajo.2020.05.027

network and is critical for metabolic support of retinal pigment epithelium and photoreceptors, by supplying oxygen and nutrients and removing metabolic wastes.[10,11] A typical single en face CC OCTA image has a grainy appearance of alternating white and black pixels, and it is difficult to discern the capillary detail. This is thought to be due to the limited resolution of current OCTA technology, noise, as well as a dynamic aspect of the CC circulation. For example, at any given time a capillary segment may be closed and/or may not show flow.[12] These dynamic changes have implications for the repeatability of CC FD measurements because the percentage of CC with flow may vary over time. To address this issue, we previously proposed averaging of multiple en face OCTA images of the CC to achieve more stable and repeatable measurements.[13,14] In addition, averaged CC images show a greater resemblance to the histologic appearance of the CC.[13,14] It should be noted that a limitation of the averaging approach is that the dynamic information is lost, and the resultant image is a map of the "structure of the flow." In addition, although the averaged image may resemble histology, it has not been validated against histology and thus may not be the true CC. In fact, as many research groups and instrument manufacturers utilize an en face slab from a position deeper than the physical location of the CC (thereby imaging the projection artifact from the CC), the resultant image is almost certainly not only the CC, but is likely confounded by artifact from various other structures. Having said that, quantitative assessments of this "CC-like" structure have provided new insights into normal aging and various macular diseases.[7–9,12,15–19]

A significant challenge with current CC quantitative assessments is that the optimal setting for visualization and quantification of the CC have yet to be established. Various groups have used a variety of settings with different axial slab positions, different reference offsets, and different thresholding approaches.[7–9,12,15–20] As there is no true or universally accepted ground-truth validation standard available at present, it is difficult to convincingly argue that one approach is better than another. In the absence of such validation, an alternate approach may be to select a "CC" processing strategy that yields the most repeatable results. If a highly repeatable measurement can be obtained and this measurement correlates with another disease variable of interest, this "CC" measurement may still be a valuable biomarker. In this study, we attempt to better define the optimal slab setting, offset reference, and the Phansalkar local thresholding radius for achieving the most repeatable CC FD% measurements in healthy eyes.

METHODS

THIS PROSPECTIVE, CROSS-SECTIONAL STUDY WAS CONducted at the Doheny-UCLA Eye Centers between December 2017 and March 2019. SS OCTA images were obtained from healthy volunteers. This study was approved by the UCLA Institutional Review Board and adhered to the tenets of the Declaration of Helsinki and the Health Insurance Portability and Accountability Act. Written informed consent was obtained from all subjects prior to enrollment in the study. All subjects underwent a comprehensive ophthalmic examination including slit lamp biomicroscopy, tonometry, and SS OCTA. Healthy subjects with a normal examination, no history of eye disease, and a normal structural OCT of the macula were enrolled. Subjects were excluded for any refractive error greater than 3 diopters (D). Subjects with systemic diseases such as diabetes mellitus, hypertension, and dyslipidemia were also excluded.

• **IMAGING:** Subjects underwent SS OCTA imaging with the PLEX Elite 9000 device (Carl Zeiss Meditec Inc, Dublin, California, USA), operating at 100,000 A-scans/second. Both eyes of each subject were imaged after pupil dilation to obtain OCTA volume scan sets with sufficient image quality (signal strength index > 7) and without motion artifact that fulfilled the acceptance criteria of the Doheny Image Reading Center.[8,9,21] All eyes were scanned 4 times using a 3×3-mm scan protocol centered on the fovea. Each 3 × 3-mm volume scan consisted of 300 A-scans per B-scan, repeated 4 times at each of the 300 B-scan positions.

• **MEASUREMENT OF FLOW DEFICIT IN EN FACE CC IMAGES:** The en face CC-OCTA images were generated in 3 different axial positions using the Max projection: a 10-μm-thick slab starting 11, 21, and 31 μm posterior to the automatically segmented retinal pigment epithelial band centerline. The Max projection averages the 5 highest-flow pixel values to generate the en face CC images and is the device's default setting for the CC. The projection removal function of the device software was applied, which removed the flow signal cast by the overlying retinal vessels from the CC slab, so that the retinal vessels did not confound the CC assessment. The resultant CC-OCTA image is isotropic, with a separation of 10 μm between A-scans. The en face CC-OCTA images were binarized for quantitative analysis of FDs using the Phansalkar local thresholding method (radius: 15 pixels, 43.94 μm) in ImageJ software, version 1.50 (National Institutes of Health, Bethesda, Maryland, USA; available at http://rsb.info.nih.gov/ij/index.html) as previously described.[8,9,12,15] The extent of FD was computed as a percentage of the total scan area in each scan image. Figure 1 shows representative en face CC-OCTA images from a normal eye and corresponding binarized CC images from the 3 slab positions.

• **MODULATION OF PROJECTION METHOD, OFFSET REFERENCE, AND PHANSALKAR LOCAL THRESHOLDING RADIUS:** The entire analysis was repeated after modifying specific settings. First, the Sum projection, which generates the en face CC image by the summation of all flow pixel values for each A-scan, was used instead of the Max

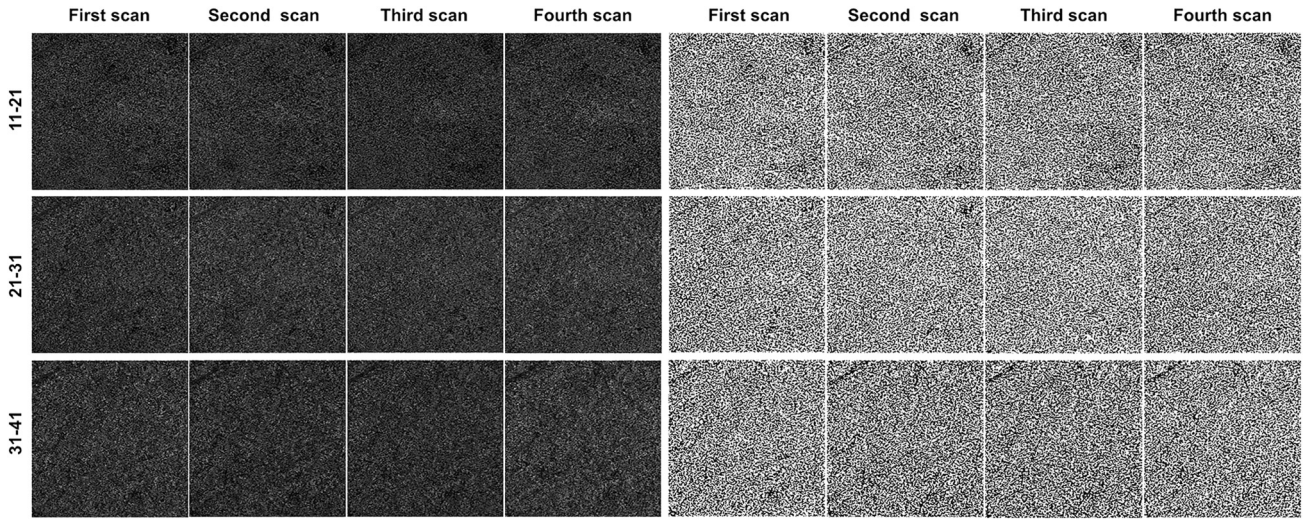

FIGURE 1. Representative 3 × 3-mm en face choriocapillaris OCTA images with 3 different slab positions. All 4 consecutive scans are shown using the Max projection (left) with their corresponding binarized images using the Phansalkar local thresholding method with a radius of 43.94 μm (15 pixels) (right). The retinal pigment epithelium band was used as the reference of slab offset. OCTA = optical coherence tomography angiography.

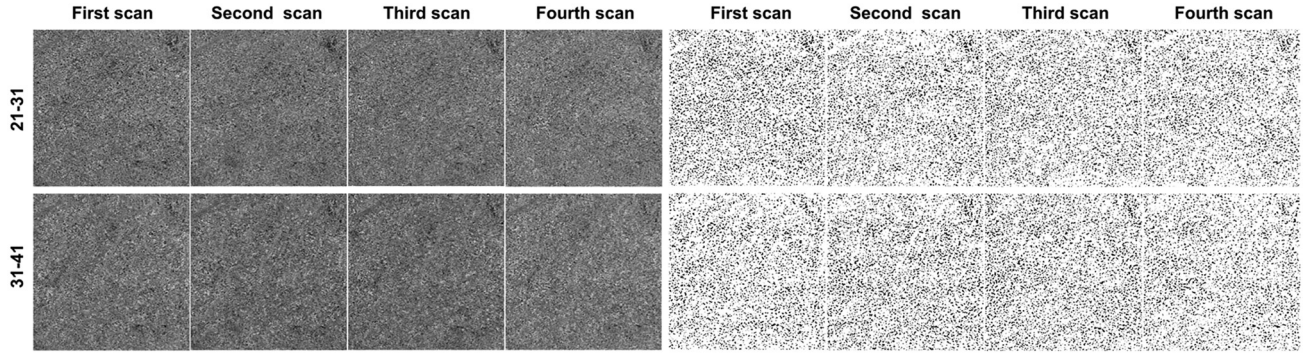

FIGURE 2. Representative 3 × 3-mm en face choriocapillaris OCTA images with 2 different slab positions. All 4 consecutive scans are shown using the Sum projection (left) with their corresponding binarized images using the Phansalkar local thresholding method with a radius of 43.94 μm (15 pixels) (right). The retinal pigment epithelium band was used as the reference of slab offset. OCTA = optical coherence tomography angiography.

projection (Figure 2). Second, the retinal pigment epithelial fit was used as the reference position for the offset of the slabs rather that the retinal pigment epithelial band centerline (Figure 3). The retinal pigment epithelial fit is intended to approximate the position where the retinal pigment epithelial centerline should normally be located in eyes where the axial position of the retinal pigment epithelium is displaced by disease,[8,9,15,21] such as eyes with drusen where the retinal pigment epithelial band may have an undulating contour. In such cases, the retinal pigment epithelial fit is crucial as it creates a relatively flat surface from which an offset slab can be taken. In normal eyes where the retinal pigment epithelium is a relatively flat monolayer, the retinal pigment epithelial fit should theoretically mirror the location of the retinal pigment epithelial band centerline, though that is not always the case because of variability in the performance of the retinal pigment epithelial fit segmentation algorithm. The geometry and not just the separation between the center of the retinal pigment epithelial band and Bruch membrane may be relevant, because the device attempts to identify the line of maximum brightness in the retinal pigment epithelial band (which is generally the middle of the retinal pigment epithelial band) and then generates the retinal pigment epithelial fit through a flattening process. This can create deviations from the retinal pigment epithelial band centerline in normal eyes, creating this discrepancy between the retinal pigment epithelial fit and the retinal pigment epithelial band. Third, we modified the radius value of the Phansalkar local thresholding method to a smaller value of 14.65 μm (5 pixels in a 3 × 3-mm 300 × 300 A-

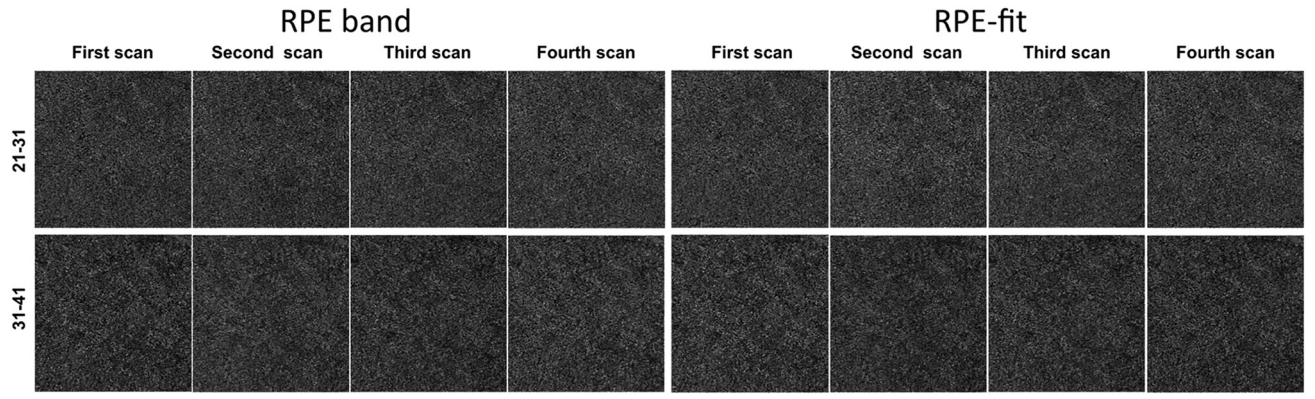

FIGURE 3. Representative 3 × 3-mm en face choriocapillaris OCTA images with 2 different slab positions. All 4 consecutive scans are shown using the RPE band (left) and RPE fit (right) as the reference of slab offset. The Max projection was applied. The different en face OCTA images were generated in the same slab position and scan acquisition. OCTA = optical coherence tomography angiography; RPE = retinal pigment epithelium.

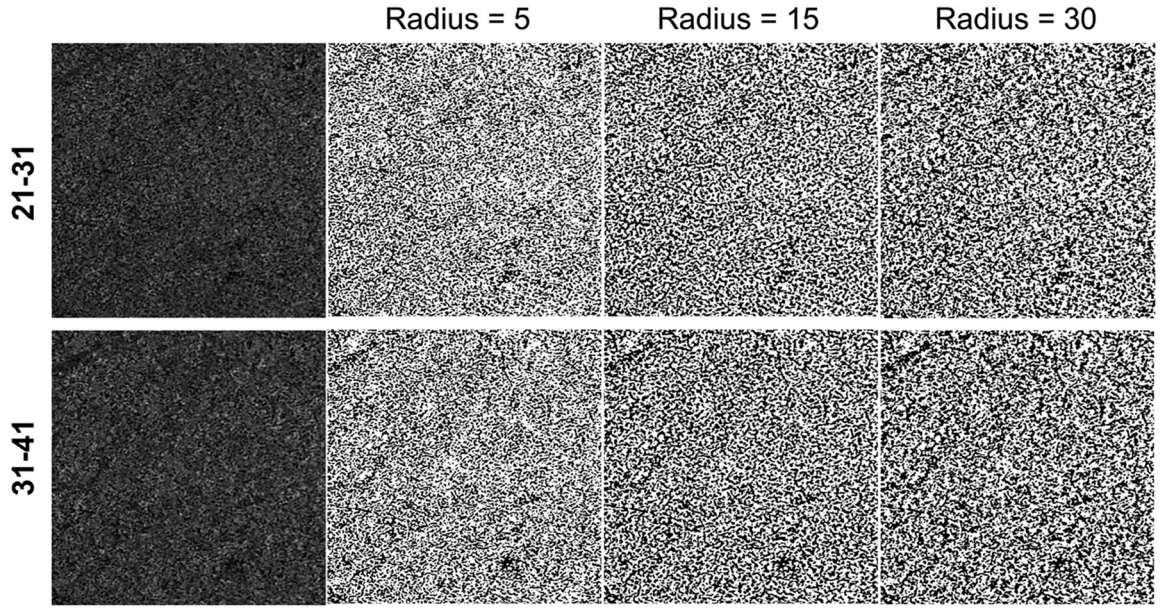

FIGURE 4. Representative, binarized CC images generated by Phansalkar local thresholding method with different radius values (shown here in pixels) with 2 different slab positions. The Max projection was applied and retinal pigment epithelium band was used as the reference of slab offset. Note the significant difference in the size of the flow deficits (black pixels) with increase in the radius. OCTA = optical coherence tomography angiography.

scan image) and a larger value of 87.88 μm (30 pixels) (Figure 4).

• **STATISTICAL ANALYSIS:** The repeatability of the CC FD% among the 4 consecutive acquisitions was assessed using both intraclass correlation coefficient (ICC) and coefficient of variation (CV). The ICC is the correlation between 4 variables measured at different time points, showing their resemblance in a group. As it approaches 1, the repeatability of the measurement increases proportionally. The CV is the ratio of the standard deviation and the mean, and a value closer to 0 is a reflection of higher repeatability. Generalized estimating equations were used to adjust for correlations between 2 eyes of the same subject. Statistical analyses were performed using SPSS Statistics version 20 (IBM, Armonk, New York, USA). A P value of $<.05$ was considered to be statistically significant.

TABLE 1. Repeatability of Choriocapillaris Flow Deficits in 3 Slab Positions Using the Retinal Pigment Epithelial Band Centerline as the Offset Reference With Max Projection

	First Measured CC FD Values (%, Mean ± SD)	Second Measured CC FD Values (%, Mean ± SD)	Third Measured CC FD Values (%, Mean ± SD)	Fourth Measured CC FD Values (%, Mean ± SD)	Mean CC FD Values (%, Mean ± SD)	ICC	CV
11-21-μm slab	59.3 ± 11.8	60.5 ± 10.8	58.9 ± 10.9	59.1 ± 10.3	59.4 ± 10.8	0.963 (0.932-0.982) $P < .001$	0.05
21-31-μm slab	43.0 ± 8.6	43.0 ± 8.4	42.6 ± 7.7	42.2 ± 6.9	42.7 ± 7.8	0.975 (0.954-0.988) $P < .001$	0.05
31-41-μm slab	40.6 ± 4.7	39.9 ± 4.7	40.7 ± 3.7	39.6 ± 4.4	40.2 ± 4.4	0.911 (0.834-0.957) $P < .001$	0.05

CC = choriocapillaris, CV = coefficient of variation, FD = flow deficit, ICC = intraclass correlation coefficient.
Phansalkar radius of 43.94 μm (15 pixels) was applied.

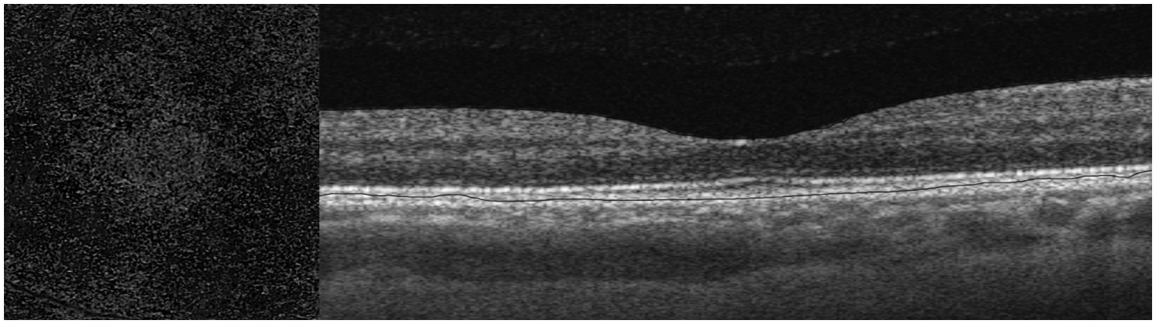

FIGURE 5. Representative en face choriocapillaris OCTA image showing hypointense regions in the 11-21-μm slab using the Max projection (left) and B-scan image showing the automated segmentation line of retinal pigment epithelium band as the reference for slab offset (right). The hypointense regions are seen parafoveally, especially inferiorly, and are due to subtle errors in the automated segmentation (gray line in B-scan). OCTA = optical coherence tomography angiography.

RESULTS

TWENTY-FOUR EYES OF 12 HEALTHY SUBJECTS (8 MALES AND 4 females) were included in this analysis. The mean age was 36.4 ± 5.6 years (range 27-43 years). The mean CC FD%s of the 11-21-, the 21-31-, and the 31-41-μm slabs using the primary (instrument default) processing approach (Max projection, retinal pigment epithelial centerline as the offset reference, Phansalkar radius of 43.94 μm) were 59.4% ± 10.8%, 42.7% ± 7.8%, and 40.2% ± 4.4%. The ICCs and CVs of the CC FD% for the 11-21-, 21-31-, and 31-41-μm slabs were 0.963, 0.975, and 0.911 and 0.05, 0.05, and 0.05, respectively (Table 1).

• **HYPOINTENSE REGIONS IN EN FACE OCTA IMAGES:** In some cases, slabs close to the retinal pigment epithelial band (ie, the 11-21-μm slab), demonstrated a hypointense region caused by inadvertent inclusion of the retinal pigment epithelial band in the slab (Figure 5). We have reported this finding previously, and this has the potential to artificially increase the CC FD%.[20] To address this confounder and better understand its impact, we repeated all analyses excluding those eyes that demonstrated these regions in any of the scans. Only 6 eyes (age 25.6 ± 3.8 years) were included in this exploratory analysis as most eyes had evidence of this hypointense region in at least 1 of the scans with the superficial (11-21-μm) slab. The Max projection and retinal pigment epithelial band centerline were used to generate the en face CC OCTA images for this analysis, and the CC FD% was assessed in the binarized image using all 3 different Phansalkar local thresholding radii (14.65, 43.94, and 87.88 μm). The ICCs and CVs of the 11-21-, 21-31-, and 31-41-μm slabs were, respectively, 0.792, 0.926, and 0.754 and 0.11, 0.10, and 0.11 for a 14.65 μm (5 pixel) radius; 0.700, 0.929, and 0.782 and 0.07, 0.06, and 0.06 for the 43.94 μm (15 pixel) radius; and 0.788, 0.935, and 0.795 and 0.07, 0.06, and 0.06 for the 87.88 μm (30 pixel) radius, respectively (Table 2). Again, the 21-31-μm slab yielded the most repeatable CC FD% measurement.

As most of the cases were confounded with the hypointense region when the 11-21-μm slab was used, this slab could not meaningfully be included in further analyses of

TABLE 2. Repeatability of Choriocapillaris Flow Deficits in 3 Slab Positions in 6 Eyes Without Hypointense Regions Using 3 Phansalkar Local Thresholding Radii

	CC FD% (Mean ± SD)				ICC			CV		
	R = 14.65 μm (5 Pixels)	R = 43.94 μm (15 Pixels)	R = 87.88 μm (30 Pixels)	*P* Value	R = 14.65 μm (5 Pixels)	R = 43.94 μm (15 Pixels)	R = 87.88 μm (30 Pixels)	R = 14.65 μm (5 Pixels)	R = 43.94 μm (15 Pixels)	R = 87.88 μm (30 Pixels)
11-21-μm slab	45.3 ± 6.5	45.3 ± 4.8	47.7 ± 4.6	<.001	0.792 (0.254-0.968)	0.700 (−0.075 to 0.953)	0.788 (0.243-0.967)	0.11	0.07	0.06
					P = .008	*P* = .032	*P* = .009			
21-31-μm slab	28.4 ± 5.5	35.7 ± 4.4	36.8 ± 4.0	<.001	0.926 (0.737-0.989)	0.929 (0.747-0.989)	0.935 (0.766-0.990)	0.10	0.06	0.05
					P < .001	*P* < .001	*P* < .001			
31-41-μm slab	31.3 ± 4.9	38.9 ± 3.5	39.6 ± 3.5	<.001	0.754 (0.121-0.962)	0.782 (0.222-0.966)	0.795 (0.268-0.968)	0.11	0.06	0.05
					P = .016	*P* = .010	*P* = .008			

CC = choriocapillaris, CV = coefficient of variation, FD = flow deficit, ICC = intraclass correlation, OCTA = optical coherence tomography angiography, R = radius.
Retinal pigment epithelial band centerline as offset reference and Max projection were applied.

the repeatability of CC FD% measurement (see below). Regardless, the high frequency of hypointense artifact with this slab would appear to limit its feasibility for clinical practice, where manual adjustments are not practical.

• **REPEATABILITY OF MAX VS SUM PROJECTION:** The Sum projection yielded generally brighter CC images that seemed qualitatively different (Figure 2), compared with the Max projection images. The mean CC FD%s of the 21-31-μm and 31-41-μm slabs were 17.8% ± 6.0% and 13.3% ± 3.7%, respectively, which were significantly different from those of the corresponding slab position using the Max projection ($P < .01$ in all). The ICCs and CVs using the Sum projection for the 2 slabs were 0.916 and 0.766 and 0.15 and 0.19, respectively (Table 3). The Max projection consistently yielded more repeatable results compared with the Sum for both slab positions: 0.975 vs 0.916 (ICC) and 0.05 vs 0.15 (CV) in the 21-31-μm slab and 0.911 vs 0.766 (ICC) and 0.05 vs 0.19 (CV) in the 31-41-μm slab, respectively. Of note, the 21-31-μm slab was consistently the most repeatable for CC FD% measurement from en face OCTA images generated by both Max and Sum projection approaches. Tables 1 and 3 summarize the 4 consecutive CC FD% measurements and their repeatability values (the ICCs and CVs) for the 2 deeper slab positions using the Max and Sum projections.

• **REPEATABILITY OF RETINAL PIGMENT EPITHELIAL BAND CENTERLINE OR RETINAL PIGMENT EPITHELIAL FIT AS THE OFFSET REFERENCE:** Using the retinal pigment epithelial fit as the reference, the en face images in the 2 slab positions were obtained using the Max projection, and then the CC FD% was measured using a Phansalkar local thresholding radius of 43.94 μm (Figure 3). The mean CC FD%s of the 21-31- and 31-41-μm slabs were 40.3% ± 6.0% and 40.0% ± 3.4%, respectively, which were not significantly different from those obtained using the retinal pigment epithelial band centerline as the reference. The ICCs and CVs from the retinal pigment epithelial fit were 0.907 and 0.802 and 0.06 and 0.06, respectively, which indicated lower repeatability values in 2 slab positions compared with those obtained using the retinal pigment epithelial band centerline as the reference (retinal pigment epithelial fit vs retinal pigment epithelial band centerline: 0.907 vs 0.975 [ICC] and 0.06 vs 0.05 [CV] for the 21-31, and 0.802 vs 0.911 [ICC] and 0.05 vs 0.06 [CV] for the 31-41-μm slabs, respectively; Table 4). The 21-31-μm slab again yielded the most repeatable CC FD % measurement even when the retinal pigment epithelial fit was used in this cohort of normal eyes.

• **REPEATABILITY OF DIFFERENT PHANSALKAR LOCAL THRESHOLDING RADII:** Using the retinal pigment epithelial band centerline as the offset reference and the Max projection algorithm, en face CC OCTA images were generated in the 2 slab positions. For CC FD%

TABLE 3. Repeatability of Choriocapillaris Flow Deficits in 2 Slab Positions Using the Retinal Pigment Epithelial Band Centerline as the Offset Reference With Sum Projection

	First Measured CC FD Values (%, Mean ± SD)	Second Measured CC FD Values (%, Mean ± SD)	Third Measured CC FD Values (%, Mean ± SD)	Fourth Measured CC FD Values (%, Mean ± SD)	The Mean CC FD Values (%, Mean ± SD)	ICC	CV
21-31-μm slab	18.6 ± 7.1	17.9 ± 6.5	16.9 ± 5.1	17.9 ± 5.5	17.8 ± 6.0	0.916 (0.844-0.960) $P < .001$	0.15
31-41-μm slab	13.5 ± 4.2	13.7 ± 3.7	13.2 ± 2.8	12.7 ± 4.0	13.3 ± 3.7	0.776 (0.583-0.893) $P < .001$	0.19

CC = choriocapillaris, CV = coefficient of variation, FD = flow deficit, ICC = intraclass correlation coefficient.
Phansalkar radius of 43.94 μm (15 pixels) was applied.

TABLE 4. Repeatability of Choriocapillaris Flow Deficits in 2 Slab Positions Using the Retinal Pigment Epithelial Fit as the Offset Reference With Max Projection

	First Measured CC FD Values (%, Mean ± SD)	Second Measured CC FD Values (%, Mean ± SD)	Third Measured CC FD Values (%, Mean ± SD)	Fourth Measured CC FD Values (%, Mean ± SD)	Mean CC FD Values (%, Mean ± SD)	ICC	CV
21-31-μm slab	39.7 ± 3.8	39.6 ± 6.1	40.1 ± 6.4	41.1 ± 7.3	40.3 ± 6.0	0.907 (0.827-0.956) $P < .001$	0.06
31-41-μm slab	39.3 ± 3.0	40.5 ± 3.5	40.0 ± 3.0	40.0 ± 4.2	40.0 ± 3.4	0.802 (0.631-0.905) $P < .001$	0.06

CC = choriocapillaris, CV = coefficient of variation, FD = flow deficit, ICC = intraclass correlation coefficient.
Phansalkar radius of 43.94 μm (15 pixels) was applied.

computation, the resultant CC OCTA images were binarized using Phansalkar local thresholding radii of 14.65 μm (5 pixels) and 87.88 μm (30 pixels) (Figure 4). Using a radius of 14.65 μm, the mean CC FD%s of the 21-31- and 31-41-μm slabs were 38.5% ± 10.2% and 35.2% ± 6.1%, respectively. Using a radius of 87.88 μm, the mean CC FD%s were 42.9% ± 7.5% and 40.7% ± 4.1%. These CC FD%s significantly differed in the 21-31- and 31-41-μm slab positions among 3 radius values (14.65, 43.94, and 87.88 μm) ($P < .001$ in both; Table 4). The ICCs and CVs of the 2 slab positions were 0.960 and 0.912, and 0.08 and 0.08 using a 14.65 μm radius, respectively, and 0.958 and 0.894, and 0.05 and 0.05 using a 87.88 μm radius (Table 5). Again, as a consistent finding across our study, the 21-31-μm slab was the most repeatable regardless of the Phansalkar local thresholding radius.

DISCUSSION

IN THIS STUDY IN WHICH WE MODULATED SEVERAL PARAMeters relevant to processing OCTA images for quantitative CC assessment, we observed that the repeatability of CC FD% measurements in healthy eyes could be significantly affected by the CC slab selection, the offset reference, the projection method, and the local thresholding radius. Of note, regardless of the projection or local thresholding method used, we observed that a 10-μm slab positioned 21-31 μm below the retinal pigment epithelial band centerline yielded the most repeatable results. In addition, for healthy eyes, offsets relative to the retinal pigment epithelial band centerline, and OCTA images generated based on a Max projection, yielded the most repeatable results. In addition to repeatability, our findings also show that the absolute CC FD% can vary dramatically depending on the processing parameters used, emphasizing the need for a consistent processing approach across a study. If a consistent approach is used, we observed that a CV of 5% could be achieved for CC FD% measurements.

The CC has become accessible as a result of OCTA. Although the CC can sometimes be appreciated with high-quality indocyanine green angiography, the resolution of conventional indocyanine green angiography is generally insufficient to visualize the intercapillary spaces. Even with OCTA, resolution is an issue, though semblance of what appears to be CC architecture can be visualized on averaged images. This becomes more easily apparent with

TABLE 5. Repeatability of Choriocapillaris Flow Deficits in 2 Slab Positions Using 3 Phansalkar Local Thresholding Radii

	CC FD% (Mean ± SD)				ICC			CV		
	R = 14.65 μm (5 Pixels)	R = 43.94 μm (15 Pixels)	R = 87.88 μm (30 Pixels)	*P* Value	R = 14.65 μm (5 Pixels)	R = 43.94 μm (15 Pixels)	R = 87.88 μm (30 Pixels)	R = 14.65 μm (5 Pixels)	R = 43.94 μm (15 Pixels)	R = 87.88 μm (30 Pixels)
21-31-μm slab	38.5 ± 10.2	42.7 ± 7.8	42.9 ± 7.5	<0.001	0.960 (0.926-0.981) $P < .001$	0.975 (0.954-0.988) $P < .001$	0.958 (0.922-0.980) $P < .001$	0.08	0.05	0.05
31-41-μm slab	35.2 ± 6.1	40.2 ± 4.4	40.7 ± 4.1	<0.001	0.912 (0.836-0.958) $P < .001$	0.911 (0.834-0.957) $P < .001$	0.897 (0.809-0.951) $P < .001$	0.08	0.05	0.05

CC = choriocapillaris, CV = coefficient of variation, FD = flow deficit, ICC = intraclass correlation, OCTA = optical coherence tomography angiography, R = radius.
Retinal pigment epithelial band centerline as offset reference and Max projection were applied.

higher-resolution AO OCTA devices.[22] Although the CC images obtained from these devices may more closely approximate the putative ground truth, these higher-resolution instruments are expensive and not commercially available. Thus, most existing CC OCTA research has been performed with spectral domain or SS OCTA devices that are commercially available. Although it should be acknowledged that there is no histologic validation that what is being imaged corresponds precisely to the anatomic CC, the "CC" as visualized by current OCTA approaches does seem to have value in our understanding of various diseases.[8,9,17,18,21,23–26] Although the CC can be visualized using spectral domain OCTA, there may be advantages of deeper-penetrating SS OCTA in the setting of diseases that may further attenuate the OCT signal, such as drusen in the setting of age-related macular degeneration.[4] On the other hand, the deeper penetration of SS OCTA may create more projection artifact in the choroid, which may be of particular relevance when deeper slabs are used for CC imaging.

Despite these many potential issues, qualitative assessments of the integrity of the CC on OCTA have been of value, and have been shown to potentially be useful for distinguishing white dot syndromes such as placoid disorders, which demonstrate CC ischemia, from multiple evanescent white dot syndrome, which do not exhibit CC alteration.[23] Although qualitative assessment is of value, to fully exploit the information potentially encoded in the CC on OCTA, quantitative assessment is essential. Quantitative CC studies on OCTA have already shown progressive worsening of CC flow with age, with increasing CC FDs, especially centrally.[19,27] Investigators have also shown worsening CC FDs with increasing severity of age-related macular degeneration,[28] and have demonstrated a correlation between the severity of CC FD and the enlargement rate of geographic atrophy.[29] Given the potential importance of quantitative CC data, establishing the repeatability of this measure and optimal processing approaches to maximize repeatability would appear to be of value and served as the principal rationale for our study.

Although all current OCTA instruments obtain repeated scans in the same location to contrast for motion, they differ in the details of their processing scheme (amplitude vs phase decorrelation vs mixed/complex), and much of this is proprietary and not available to the user. Even within the same device, differences in signal from one scan to the next can have significant impact on measurements.[30] For the CC, there are additional issues related to selection of parameters for processing the CC data. In our study, we observed that the Max projection approach yielded a more repeatable result compared with the Sum projection. The Max projection averages the greatest 5 flow pixel values for each A-scan in the selected slab area, whereas the Sum adds all flow pixels in the A-scan, which creates an overall brighter image. In theory, these 2 projection options should be equivalent in the

repeatability values (flow pixel values should consistently be 5 times larger in the Sum projection). In practice, however, we found the following possible causes for the observed differences. First, when the slab offset is translated from micrometers to pixels, it is rounded to the nearest integer; for some locations, this results in a 5-pixel thickness slab and in some locations to a 6-pixel slab because of the rounding. This can also produce an effect of "ridges" in the Sum projection. When generating very thin slabs like these, adding 5 vs 6 pixels in a given A-scan can produce higher differences between Sum and Average than when adding, for example, 20 vs 21 pixels. Second, when defining a 5-pixel slab where the 2 layers defining the slab are separated by 5 pixels, this actually considers 6 pixels per A-scan because the top and bottom boundaries are included in the slab generation. This may cause slight differences in the Max and Sum projection because the Max considers 5 pixels and the Sum considers 6 pixels. Third, the Sum and Max projection go through a different global normalization. This may cause the slab to have a different brightness and contrast behavior. It is hoped that this issue will be addressed in future iterations of the manufacturer's software that will create a precise 5-pixel slab for both projection approaches.

In addition to the projection method, OCTA devices allow the user to select a surface from which an en face slab may be offset. For CC assessment, there are generally 2 relevant references in the PLEX Elite 9000 device that were both evaluated in this study, the retinal pigment epithelium and the retinal pigment epithelial fit. The retinal pigment epithelial fit is intended to be an approximation of the expected location of the retinal pigment epithelial band in a normal eye, and is of particular value in eyes in which the retinal pigment epithelium is pathologically elevated (eg, by drusen), in which case the use of an retinal pigment epithelial band reference would yield a very uneven or undulating segmentation. Thus, in diseased eyes, the retinal pigment epithelial fit would generally be preferred for CC assessment,[4,8,9,15,21,26] as it would essentially flatten the reference line. Unfortunately, at present, the retinal pigment epithelial fit line in most devices does not perfectly approximate the expected retinal pigment epithelium–Bruch membrane complex position in the setting of disease, and segmentation error is a significant issue. Most commonly, when there are significant drusen or other pathology elevating the retinal pigment epithelium, the retinal pigment epithelial fit may "float" anteriorly and may be positioned substantially internal to Bruch membrane (Supplementary Figure 1; drusen eyes). Thus, reliable CC assessments in diseased eyes invariably require significant adjustment of segmentation errors. However, in healthy eyes, both the retinal pigment epithelium and retinal pigment epithelial fit are anticipated to be positioned in the middle of the retinal pigment epithelium–Bruch membrane complex ("retinal pigment epithelial band centerline"). In fact, in our inspection of the position of these lines in our normal cohort, they were positioned in nearly the same location. Yet, despite an overall similar location, we observed that at any given A-scan location, the retinal pigment epithelial fit could be positioned a few micrometers anterior or posterior to the retinal pigment epithelial band line even in healthy eyes (Supplementary Figure 2; healthy eyes). This inconsistency in the retinal pigment epithelial fit location likely explains the better repeatability observed when using the retinal pigment epithelial band centerline as the offset reference compared with the retinal pigment epithelial fit in our study. This suggests that the algorithm to generate the retinal pigment epithelial fit is more susceptible to scan-to-scan variation. It should be emphasized, however, that we can only draw this conclusion in normal eyes. Despite the apparent worse repeatability, there may be no choice but to use the retinal pigment epithelial fit in diseased eyes to compensate for undulations in the retinal pigment epithelial contour.

A final parameter evaluated in our analysis was the Phansalkar local thresholding radius. Investigators have shown that the size of the radius can impact the CC FD % measurement and its repeatability.[31] Some have suggested that radius needs to be modified based on the expected intercapillary spacing, but this is challenging as the spacing varies depending on the region. Regardless, there is no consensus on the optimal radius. Our study was not designed to establish the optimal radius, but we did seek to determine whether the Phansalkar local thresholding radius could impact which slab was most repeatable. Although we confirmed that changing the radius significantly impacted the absolute CC FD% values, we still observed that the most repeatable results were observed with the 21-31-μm slab. However, among the radii we evaluated, although there were numerical differences among the ICCs, these were not statistically significant.

With regard to slab position, which was the main focus of our study, researchers have used various slabs because of a lack of ground truth validation against histology.[4,8,15–19,21,23,24,26–29] Histologically, the optimal slab position for the CC FD% assessment should presumably be located just below Bruch membrane and extend to the inner border of the Sattler layer. Reliable segmentation of Bruch membrane, however, is challenging. Automated methods are error-prone, and even manual segmentation/adjustment is a challenge as a single-pixel displacement yields a 2-μm difference. With human "mouse shake," avoiding a single-pixel error for every A-scan of every B-scan will be difficult. In addition, the outer border of the CC may not be located a constant offset from Bruch membrane, which introduces further inaccuracies in achieving "true" anatomic CC segmentation. We did observe in this study and in a prior study[20] that a shift in slab position could yield significant absolute quantitative differences in CC FD%, so consistent slab selection is essential for any investigation. One might assume that the optimal slab is thin (10-μm) and located just below the Bruch membrane

in the expected anatomic location of the CC. The PLEX Elite 9000 device automatically segments the middle of the retinal pigment epithelium–Bruch membrane complex as a reference line. Therefore, to position the slab immediately below the retinal pigment epithelium–Bruch membrane complex, one may need to account for the thickness of Bruch membrane (2-4 μm) as well as the retinal pigment epithelium (14 μm).[32,33] However, the visualization of the CC in OCTA may not be as simple as positioning a slab in the proper anatomic location. In fact, the CC slab positions that many researchers have used in prior studies, as well as the default settings of most devices, have generally been deeper (eg, the 31-41-μm and the 29-49-μm slab) than that predicted by anatomy.[4,8,9,12,16–24,26–29] The theoretical advantage of deeper slabs is that they are less prone to inadvertent inclusion of the retinal pigment epithelium–Bruch band (and a resultant hypointense region), which would otherwise need to be mitigated by tedious and meticulous correction of the segmentation. In fact, we did observe such hypointense regions in our 11-21-μm slab (Figure 5) in many eyes. The disadvantage of a deeper slab is that one is likely imaging projection artifact from the CC rather than the actual flow in the CC. In addition, the "CC" image in this case may be "polluted" by noise from other choroidal structures in this anatomic location. Thus, this deeper slab may be better termed an "inner choroidal slab," and we would propose the use of this term in future studies. The potential introduced by using a deeper slab is apparent when viewing the structural OCT en face images from these locations, which can show a variegated intensity pattern (Supplementary Figure 3). Despite these potential limitations, however, we found that the most repeatable is the 21-31-μm slab offset relative to the retinal pigment epithelial band centerline. It should be noted that although the 11-21-μm slab is the most homogenous, the variegation in the 21-31-μm structural OCT slab (Supplementary Figure 3) is relatively mild (compared to the 31-41-μm slab), and thus the 21-31-μm may be a good compromise. Regardless of whether such a deeper slab is measuring the CC or some "polluted" CC, we would argue that this would be the preferred slab for use in research if it is most repeatable and still correlates with other markers of interest.

Although we evaluated many parameters that can impact the repeatability of CC assessments, it is important that other factors can also influence the repeatability of the CC FD% measurement. One very important consideration is signal strength. We included only images with a signal strength index >7 to mitigate this, but we have shown that even with good signal, small differences in signal can impact vessel density measurements.[30] Another consideration is the position of the eye. Tilting of OCT scans can alter the detection of CC flow by influencing the projection of superficial flow onto the deeper layers.[34] For this reason, we paid great attention to the centration of the scan beam in the pupil during acquisition. The binarization method including local or global thresholding and brightness/contrast adjustment also may be factors affecting the repeatability of the CC FD% measurement.[35] Proper adjustment of the thresholding and brightness and contrast settings that generate binarized images with a qualitative resemblance to the flow image should be considered for accurate and repeatable CC FD% measurements. Finally, other problems such as motion artifact and segmentation error can also affect the reliability of CC FD% measurement and must also be scrutinized for. A careful interpretation of the repeatability data is also needed in situations where there is a discrepancy between ICC and CVs. In our study, both the ICC and CV demonstrated that the 21-31-μm slab was most repeatable in most experiments. However, when assessing different Phansalkar radii, R = 14.65 μm had higher ICC values than R = 87.88 μm, but worse CV values. In such a situation, we would propose that the ICC would be more reliable than the CV, because of inherent potential limitations in the CV. Specifically, a large mean could result in a small CV even if there is significant lot variation.

Our study has other limitations that should also be considered when assessing our results. First, although Max projection and a 21-31-μm slab offset relative to the retinal pigment epithelial band centerline reference yielded the most repeatable results in our study, it does not mean these are the optimal parameters. There may be settings that we did not explore which could yield even better results. Moreover, this study was focused only on repeatability of slabs and not on accuracy/sensitivity. The sensitivity of a particular slab for discriminating a clinical outcome of interest may need to be established for each clinical scenario. However, the deeper slabs evaluated in our study have been used in prior publications and have been found to be predictive of other clinical parameters of interest.[4,8,9,12,16–24,26–29,36] The repeatability of these various slabs will also need to be confirmed for specific disease applications. For example, the repeatability may not be as good in myopic eyes with thin choroids. On the other hand, we can infer that if our method is used in normal eyes, we can expect a high level of repeatability with a CV of 5%. That could be of use in powering future studies, especially longitudinal analyses of normal and aging eyes. A second limitation of our study is its relatively small sample. However, repeated imaging is challenging for subjects, and the multiple permutations creates an exhaustive analysis. Despite the limited sample, we were still able to find several significant differences. Third, our study only included healthy eyes. As we have noted, in diseased eyes, the retinal pigment epithelial fit with adjustment of any segmentation errors would likely have to be used. Although we expect that many of our observations (eg, absolute slab position) would still apply if the segmentation was corrected appropriately, parameters such as the Phansalkar local thresholding radius may need to be adjusted in the setting of disease if the disease produces large

regional variations in the intercapillary spacing. On the surface, the values of CC FD% assessed by our approach (Max projection, retinal pigment epithelial centerline as the offset reference and Phansalkar radius of 43.94 μm) appear to be somewhat similar to those reported by previous histologic study by Ramarattan and associates.[37] This study indicated that the capillary density was approximately 60% for the third decade of age with a capillary diameter of approximately 10 μm, which translates to a CC FD of 40% by histology. However, considering the lateral resolution of our OCT device of approximately 20 μm and possible shrinkage artifacts during histologic preparation, one might anticipate that CC FD% measured from the OCTA device may be significantly smaller, though this is difficult to estimate precisely. Future adaptive optics-based OCTA and especially indocyanine angiography imaging may provide an accurate ground truth reference. Although there may be absolute differences between our OCTA processing approach and histology, these OCTA values may still show relative differences between different disease conditions that can be clinically meaningful.

In summary, we observed an overall high level of repeatability of CC FD% measurement from en face CC images in normal eyes acquired by an SS OCTA device. Slab location and reference offset, projection method, and local thresholding radius could have an impact on repeatability. In this study, the use of a Max projection with a slab positioned 21-31 μm below the retinal pigment epithelial band centerline yielded the most repeatable results in healthy eyes.

FUNDING/SUPPORT: THIS STUDY RECEIVED NO FUNDING. FINANCIAL DISCLOSURES: SRINIVAS R. SADDA: ALLERGAN (CONSULtant [C], financial interest [F]), Carl Zeiss Meditec (C, F), CenterVue (C), Genentech (C, F), Heidelberg engineering (C), Iconic (C), NightstarX (C), Novartis (C), Optos (C,F), Topcon (C), and Thrombogenics (C). The other authors indicate no financial support or conflicts of interest. All authors attest that they meet the current ICMJE critera for authorship.

REFERENCES

1. Borrelli E, Sarraf D, Freund KB, Sadda SR. OCT angiography and evaluation of the choroid and choroidal vascular disorders. *Prog Retin Eye Res* 2018;67:30–55.
2. Soomro T, Talks J, Medscape. The use of optical coherence tomography angiography for detecting choroidal neovascularization, compared to standard multimodal imaging. *Eye (Lond)* 2018;32(4):661–672.
3. Gorczynska I, Migacz JV, Jonnal R, Zawadzki RJ, Poddar R, Werner JS. Imaging of the human choroid with a 1.7 MHz A-scan rate FDML swept source OCT system. In: . Opthalmic Technologies XXVII, 10045. San Francisco, CA: SPIE; 2017.
4. Lane M, Moult EM, Novais EA, et al. Visualizing the choriocapillaris under drusen: comparing 1050-nm swept-source versus 840-nm spectral-domain optical coherence tomography angiography. *Invest Ophthalmol Vis Sci* 2016;57:OCT585–OCT590.
5. Chu Z, Lin J, Gao C, et al. Quantitative assessment of the retinal microvasculature using optical coherence tomography angiography. *J Biomed Opt* 2016;21(6):066008.
6. Kim AY, Rodger DC, Shahidzadeh A, et al. Quantifying retinal microvascular changes in uveitis using spectral-domain optical coherence tomography angiography. *Am J Ophthalmol* 2016;171:101–112.
7. Zhang Q, Zheng F, Motulsky EH, et al. A novel strategy for quantifying choriocapillaris flow voids using swept-source OCT angiography. *Invest Ophthalmol Vis Sci* 2018;59(1):203–211.
8. Borrelli E, Shi Y, Uji A, et al. Topographical analysis of the choriocapillaris in intermediate age-related macular degeneration. *Am J Ophthalmol* 2018;196:34–43.
9. Nassisi M, Shi Y, Fan W, et al. Choriocapillaris impairment around the atrophic lesions in patients with geographic atrophy: a swept-source optical coherence tomography angiography study. *Br J Ophthalmol* 2019;103(7):911–917.
10. Bhutto I, Lutty G. Understanding age-related macular degeneration (AMD): relationships between the photoreceptor/retinal pigment epithelium/Bruch's membrane/choriocapillaris complex. *Mol Aspects Med* 2012;33(4):295–317.
11. Hogan MJ, Alvarado JA, Wedell JE. Histology of the human eye. Philadelphia, PA: WB Saunders; 1971.
12. Spaide RF. Choriocapillaris flow features follow a power law distribution: implications for characterization and mechanisms of disease progression. *Am J Ophthalmol* 2016;170:58–67.
13. Uji A, Balasubramanian S, Lei J, Baghdasaryan E, Al-Sheikh M, Sadda SR. Impact of multiple en face image averaging on quantitative assessment from optical coherence tomography angiography images. *Ophthalmology* 2017;124(7):944–952.
14. Uji A, Balasubramanian S, Lei J, Baghdasaryan E, Al-Sheikh M, Sadda SR. Choriocapillaris imaging using multiple en face optical coherence tomography angiography image averaging. *JAMA Ophthalmol* 2017;135(11):1197–1204.
15. Borrelli E, Uji A, Sarraf D, Sadda SR. Alterations in the choriocapillaris in intermediate age-related macular degeneration. *Invest Ophthalmol Vis Sci* 2017;58(11):4792–4798.
16. Sacconi R, Corbelli E, Carnevali A, Querques L, Bandello F, Querques G. Optical coherence tomography angiography in geographic atrophy. *Retina* 2018;38(12):2350–2355.
17. Guduru A, Al-Sheikh M, Gupta A, Ali H, Jalali S, Chhablani J. Quantitative assessment of the choriocapillaris in patients with retinitis pigmentosa and in healthy individuals using OCT angiography. *Ophthalmic Surg Lasers Imaging Retina* 2018;49(10):e122–e128.
18. Rochepeau C, Kodjikian L, Garcia MA, et al. Optical coherence tomography angiography quantitative assessment of choriocapillaris blood flow in central serous chorioretinopathy. *Am J Ophthalmol* 2018;194:26–34.
19. Zheng F, Zhang Q, Shi Y, et al. Age-dependent changes in the macular choriocapillaris of normal eyes imaged with swept-source optical coherence tomography angiography. *Am J Ophthalmol* 2019;200:110–122.

20. Byon I, Nassisi M, Borrelli E, Sadda SR. Impact of slab selection on quantification of choriocapillaris flow deficits by optical coherence tomography angiography. *Am J Ophthalmol* 2019;208:397–405.
21. Alagorie AR, Verma A, Nassisi M, Sadda SR. Quantitative assessment of choriocapillaris flow deficits in eyes with advanced age-related macular degeneration versus healthy eyes. *Am J Ophthalmol* 2019;205:132–139.
22. Kurokawa K, Liu Z, Miller DT. Adaptive optics optical coherence tomography angiography for morphometric analysis of choriocapillaris [Invited]. *Biomed Opt Express* 2017;8(3):1803–1822.
23. Wang JC, Laíns I, Sobrin L, Miller JB. Distinguishing white dot syndromes with patterns of choroidal hypoperfusion on optical coherence tomography angiography. *Ophthalmic Surg Lasers Imaging Retina* 2017;48(8):638–646.
24. Klufas MA, Phasukkijwatana N, Iafe NA, et al. Optical coherence tomography angiography reveals choriocapillaris flow reduction in placoid chorioretinitis. *Ophthalmol Retina* 2017;1(1):77–91.
25. Miyata M, Ooto S, Hata M, et al. Detection of myopic choroidal neovascularization using optical coherence tomography angiography. *Am J Ophthalmol* 2016;165:108–114.
26. Tzaridis S, Wintergerst MWM, Mai C, et al. Quantification of retinal and choriocapillaris perfusion in different stages of macular telangiectasia type 2. *Invest Ophthalmol Vis Sci* 2019;60(10):3556–3562.
27. Nassisi M, Baghdasaryan E, Tepelus T, Asanad S, Borrelli E, Sadda SR. Topographic distribution of choriocapillaris flow deficits in healthy eyes. *PLoS One* 2018;13(11):e0207638.
28. Nassisi M, Tepelus T, Nittala MG, Sadda SR. Choriocapillaris flow impairment predicts the development and enlargement of drusen. *Graefes Arch Clin Exp Ophthalmol* 2019;257(10):2079–2085.
29. Nassisi M, Baghdasaryan E, Borrelli E, Ip M, Sadda SR. Choriocapillaris flow impairment surrounding geographic atrophy correlates with disease progression. *PLoS One* 2019;14(2):e0212563.
30. Lei J, Durbin MK, Shi Y, et al. Repeatability and reproducibility of superficial macular retinal vessel density measurements using optical coherence tomography angiography en face images. *JAMA Ophthalmol* 2017;135(10):1092–1098.
31. Chu Z, Gregori G, Rosenfeld PJ, Wang RK. Quantification of choriocapillaris with OCTA: a comparison study. *Am J Ophthalmol* 2019;208:111–123.
32. Forrester J, Dick A, McMenamin P, et al. The eye: basic sciences in practice. 4th ed. Philadelphia: Elsevier; 2016.
33. Lee CJ, Vroom JA, Fishman HA, Bent SF. Determination of human lens capsule permeability and its feasibility as a replacement for Bruch's membrane. *Biomaterials* 2006;27(8):1670–1678.
34. Dolz-Marco R, Freund KB. Directional changes in tissue reflectivity may influence flow detection on optical coherence tomography angiography. *Retina* 2018;38(4):739–747.
35. Mehta N, Liu K, Alibhai AY, et al. Impact of binarization thresholding and brightness/contrast adjustment methodology on optical coherence tomography angiography image quantification. *Am J Ophthalmol* 2019;205:54–65.
36. Su L, Ji YS, Tong N, et al. Quantitative assessment of the retinal microvasculature and choriocapillaris in myopic patients using swept-source optical coherence tomography angiography. *Graefes Arch Clin Exp Ophthalmol* 2020;258:1173–1180.
37. Ramrattan RS, van der Schaft TL, Mooy CM, et al. Morphometric analysis of Bruch's membrane, the choriocapillaris, and the choroid in aging. *Invest Ophthalmol Vis Sci* 1994;35:2857–2864.